Coronary artery centerline tracking with the Morphological Skeleton Loss

Mario Viti, Hugues Talbot, Bassam Abdallah, Etienne Perot, Nicolas Gogin

CORONARY ARTERY CENTERLINE TRACKING WITH THE MORPHOLOGICAL SKELETON LOSS

Mario Viti[1,2] *Hugues Talbot*[1] *Bassam Abdallah*[2] *Etienne Perot*[2] *Nicolas Gogin*[2]

[1]CentraleSupélec, Université Paris-Saclay, Inria, F-91190 Gif-sur-Yvette France
[2]GE Healthcare, F-78530 Buc France

ABSTRACT

Coronary computed tomography angiography (CCTA) provides a non-invasive imaging solution that reliably depicts the anatomy of coronary arteries. Diagnosing coronary artery diseases (CAD) entails a clinical evaluation of stenosis and plaques, which is in turn essential for obtaining a reliable coronary-artery centerline from CCTA 3D imaging. This work proposes a centerline extraction algorithm by combining local semantic segmentation and recursive tracking. To this end we propose a Morphological Skeleton Loss (*MS_Loss*) suited for 3D centerline segmentation based on an improved morphological skeleton algorithm coupled with a resource-efficient back-propagation scheme. This work employs 225 CCTA examinations paired with manually annotated coronary-artery centerlines. This method is compared against the deep-learning state of the art in the literature using a standardized evaluation method for coronary-artery tracking.

***Index Terms*—** CT angiography, segmentation, blood vessels, deep learning.

1. INTRODUCTION

Coronary centerline extraction from CCTA is one of the fundamental phases of coronary analysis. It allows for the assessment of stenosis, the inspection of coronaries in patients with suspect CAD and the characterization of plaques [1]. Manual centerline extraction is a burdensome and time-consuming task requiring years of experience in the visual inspection of CCTA examination.

1.1. Related methods

In the earliest approaches, automatic and semi-automatic centerline extraction is based on shortest path finding [2] from manually detected seed points (extremities). These methods rely on heuristic-based cost functions that model different scenarios (stenosis, plaques, artifacts). Another approach is to obtain the centerline as a byproduct of coronary segmentation. Coronary segmentation has mainly exploited analytical and morphological vesselness filters [3, 4] or has been modeled as an optimization problem [5]. With the advent of machine learning and deep learning, heuristic-based cost functions are being replaced by supervised models that can exploit annotated data directly [6, 7, 8, 9]. The deep-learning state-of-the-art method extracts the centerline by iteratively tracking the coronary vessels using a Convolutional Neural Network for local Orientation Classification (CNN-OC) [10, 11]. This method exploits the coronary centerline alone as supervision, which is a less expensive ground-truth annotation than lumen segmentation. The centerline of coronary structures is closely related to the topological skeleton. Although not for centerline extraction, [12] proposed recently a novel topological loss (CL-Dice), which enforce connectivity in vessels by exploiting the differentiable morphological *Soft-Skeleton*. However, this formulation does not guarantee the connectivity of tubular structures. In general, the skeleton has many applications to study tubular or quasi-tubular objects. It conserves the original topology, provides 1-*d* dimensionality reduction and can be used to compute orthogonal frames. Orthogonal frames are critical in coronary inspection, enabling advanced visualization techniques [13] and automated diagnosis [14].

1.2. Skeletonization

Skeletonization is a classical process for shape simplification. In the continuous domain, the skeleton has an ideal set of properties [15]: it should be centered in the object, with the same homotopy-type as the object (in particular connectivity), and be thin (e.g. its area or volume is negligible). The grass-fire process [16] is the first historical model that produces a skeleton. In the discrete domain, these ideal properties cannot be guaranteed. In mathematical morphology, the skeleton can be defined through Lantuéjoul's formula (1), which is thin in the sense that each point of the skeleton is a neighbor of the background (non-simple points) and centered with respect to the euclidean distance transform of the object. The resulting skeleton remains, however, disconnected.

$$S(X) = \bigcup_{i \in \mathbf{N}} S_i(X) = \varepsilon_{\kappa_i}(X) \setminus \gamma_{\kappa_0}[\varepsilon_{\kappa_i}(X)], \qquad (1)$$

where γ_{κ_0} is the unit ball opening. ε_{κ_i} is the erosion with κ_i an element of a granulometric family of elementary convex structuring elements, i.e. such that $\forall(i \leq j),\ \gamma_{\kappa_i}(\kappa_j) = \kappa_j$

2. METHOD

2.1. Soft-Persistent-Skeleton

The skeletonization approach proposed in [12] is based on the discretization of Lantuéjoul's formula (1). In this case, the algorithm terminates with $S(X)$ such that $\gamma_{\kappa_0}(X) = \emptyset$. It does not guarantee that the result has the same topology as the original object. For tubular structures, this usually results in disconnections. We propose an improved skeletonization algorithm that enforces connectivity in the discrete setting (fig. 1). The resulting skeleton S from Algo. 1 however, may still contain simple points. To get a thinner output, the algorithm its reapplied $S \leftarrow$ Soft-Persistent-Skeleton(S, k). As the implementation in [12] we used a connectivity of 6 for minpool and a connectivity of 26 for maxpool. The add connection extra step allows to reconnect within a 26 connectivity neighbourhood two consecutive iterations, in practive this limits the disconnections that may happen from the result the application of erosion and subsequent opening operation.

Algorithm 1 Soft-Persistent-Skeleton

Input: I, K
  $I' \leftarrow maxpool(minpool(I))$ ▷ opening
  $S \leftarrow Relu(I - I')$ ▷ initialization
  for $i \leftarrow 0$ **to** K **do**
    $S \leftarrow max(I \odot maxpool(S), S)$ ▷ add connection
    $I \leftarrow minpool(I)$ ▷ erosion
    if $I = \emptyset$ **then** break
    end if
    $I' \leftarrow maxpool(minpool(I))$ ▷ opening
    $S \leftarrow S + (1 - S) \odot Relu(I - I')$ ▷ union
  end for
Output: S

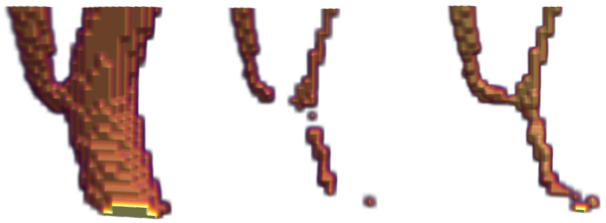

(a) (b) (c)

Fig. 1. (a) a tubular synthetic structure I. (b) its skeleton computed with *Soft-Skeleton* [12] until termination. (c) skeleton computed using Alg. 1.

2.2. *MS_Loss* and masked error

Hereafter we refer to the result of the Soft-Persistent-Skeleton applied on an argument as $SPS(*)$. We propose a Dice-like loss suited for centerline segmentation as follows:

$$MS\_Loss(X, Y) = 1 - \frac{2Prec(X, Y)Sens(SPS(X), Y)}{Prec(X, Y) + Sens(SPS(X), Y)} \quad (2)$$

Where $X : \Omega \mapsto [0, 1]$ $Y : \Omega \mapsto \{0, 1\}$ are binary valued functions defined on a continous image domain $\Omega \subseteq \mathbf{R}^3$, and $Prec(X, Y) = \sum_i X_i Y_i / \sum_i Y_i$ and $Sens(X, Y) = \sum_i X_i Y_i / \sum_i Y_i$ are scalars functions. Equation 2 requires the computation of the skeleton employing alg. 1. Although being differentiable, it is iterative. Computing gradients with back-propagation requires each iteration step to be conserved in memory. We propose approximating the gradient by exploiting the centered property of the skeleton which implies that $S(X) \leq X$, therefore $S(X) = S(X) \odot X$. By considering the segmentation as a constant factor $S(X) = S(X_{const}) \odot X$ it implies that its derivative is trivial $S(X)' = S(X_{const})$ which is indeed a term of the analytical derivative $S(X)' = S(X) + S'(X) \odot X$. For a neural network feature map $Z_\theta : \Omega \mapsto \mathbf{R}$ and the non linear activation function $\sigma(x) = 1/(1 + e^{-x})$ and given $\sigma(Z_\theta) = X_\theta$ the back-propagation development with respect to parameters θ using the chain rule follows (3). For the *Sens* function this formulation can be interpreted as a masking, and thus a change of variable of the back-propagated pixel-wise error *err*: $\frac{\partial Sens(X_\theta, Y)}{\partial X_\theta} \odot SPS(X_\theta) = err \odot SPS(X_\theta)$. The advantages of this formulation are that there is no need to fine-tune the number of iterations parameter K for the forward computation, and the back-propagation is resource-efficient (Fig, 2).

$$\begin{aligned} Sens(SPS(X_\theta), Y) &\implies \frac{\partial Sens}{\partial \theta} \\ &= \frac{\partial Sens(SPS(X_\theta), Y)}{\partial SPS(X_\theta)} \frac{\partial SPS(X_\theta)}{\partial X_\theta} \frac{\partial X_\theta}{\partial \theta} \\ &= \frac{\partial Sens(SPS(X_\theta), Y)}{\partial SPS(X_\theta)} SPS'(X_\theta) \frac{\partial X_\theta}{\partial \theta} \\ &= \frac{\partial Sens(SPS(X_\theta), Y)}{\partial SPS(X_\theta)} \odot SPS(X_\theta) \frac{\partial X_\theta}{\partial \theta} \\ &= \frac{\partial Sens(X_\theta, Y)}{\partial X_\theta} \odot SPS(X_\theta) \frac{\partial X_\theta}{\partial \theta} \end{aligned} \quad (3)$$

3. EXPERIMENTS

3.1. Topology and Homology

Given a continuous image domain $\Omega \subseteq \mathbf{R}^3$, a segmentation $I \subseteq \Omega$ has its d-dimension topological structure, called *homology class*, as an equivalence class of d-manifolds [17]. The *homology class* for a d-manifold is a countable set under I and its cardinality is the d^{th} Betti number β_d which

Method	OV	OF	OT	AI
CNN-OC [11]	0.898 ± 0.099 [0.46;0.99]	0.742 ± 0.219 [0.46;0.99]	**0.912** ± 0.099 [0.46;1.00]	0.485 ± 0.146 [0.214;0.7]
MS-Unet (ours)	**0.903** ± 0.066 [0.66;0.98]	**0.754** ± 0.212 [0.17;1.00]	0.910 ± 0.066 [0.66;0.98]	**0.460** ± 0.120 [0.204;0.65]

Table 1. Metrics (mean ± standard deviation [min; max]) on 70 CCTA examinataions of the test set compared with 2 deep learning based method: CNN-OC[11] MS-Unet, our proposal.

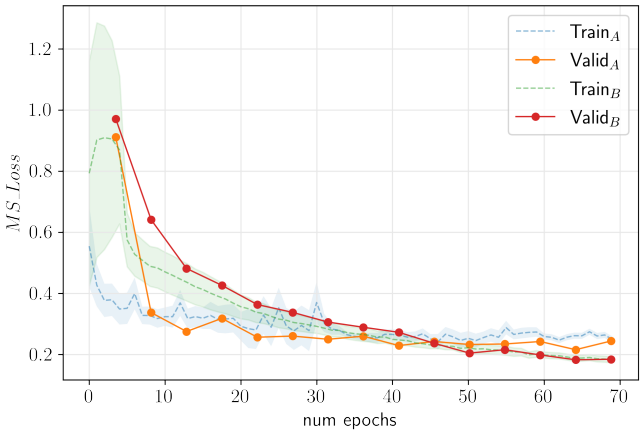

Fig. 2. MS-UNet training curves comparison without (Train$_A$, Valid$_A$) and with (Train$_B$, Valid$_B$) the masked error back-propagation. Both uses alg. 1 with same $K = 8$. In terms of training resources. Time: 5h:57m vs 4h:47m; GPU-DRAM: 17.89 GB vs 12.02 GB; for (Train$_A$/Valid$_A$) vs (Train$_B$/Valid$_B$) respectively (GeForce RTX 3070 NVIDIA).

Homotopy	β_0	β_1	β_2	E_{dist}(*,I)
I	1.3	0.1	0	0
S(I)	12.5	0	0	10.3
SPS(I)	5.2	0	0	**3.2**

Table 2. S *Soft-Skeleton* as in [12] *SPS* is the proposed Soft-Persistent-Skeleton, metrics computed on synthetic 3-*d* tubular structures I.

vanishes above the dimension of the domain Ω. For example for 3-*d* domains, β_0, β_1, β_2 correspond to the number of connected components, holes and tunnels respectively. We propose a simple check for *homotopy* (same topology) between two segmentations I and $S(I)$ is to measure the difference of their Euler number $E : \Omega \mapsto \mathbf{Z}$ as $E_{dist}(A, B) = |\inf(E(A), E(B)) - \sup(E(A), E(B))|$ which is a combination of Betti numbers: for 3-*d* objects, the Euler number is obtained as β_0+β_1-β_2.An ideal skeleton $S(I) \subseteq I \subseteq \Omega$ is homotopic and has the same *homology class* as I and therefore same Euler number. tab. 2 holds the results of this empirical check on a set of tubular synthetic structures I(fig. 1).

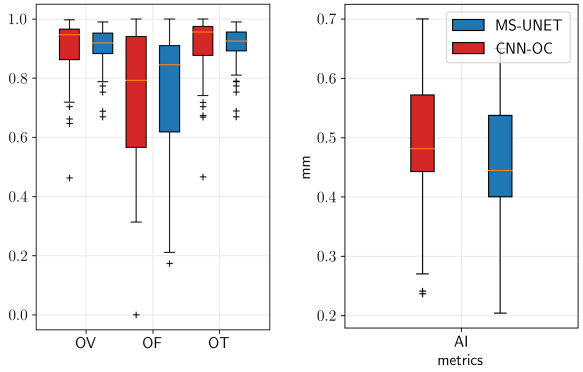

Fig. 3. Metrics measured on the test set of 70 CCTA patients with manually corrected centerlines. These metrics measure the performaces of a centerline tracker. AI metric takes account of all points not only the ones within the radius of the coronary.

3.2. Coronary Tracking

The skeletonization algorithm proposed in [12] is not suited for centerline segmentation because of the disconnected skeleton. We propose combining the *MS_Loss* and the resource-efficient back-propagation scheme to train a U-Net to segment the coronary centerline (MS-Unet). To this end, we collected a dataset of 225 CCTA examination scans paired with manually annotated centerline. These examinations are split into 100, 55, 70 for train, validation, and test, respectively. For training: as a preprocessing step, each image is resampled to 0.4 mm isotropic voxels, and a windowing (center=400, width=1000) is applied. The U-Net is fed with 32 voxels-sided cubic patches in a 64 batch. These patches are sampled around the centerline central position and augmented using random translation, rotation, scaling and skew. For the inference: the segmentation alone is not enough: extremities must be identified to isolate a single coronary centerline. We adapted the recursive tracking proposed in [9] by replacing the bayesian model with a Unet semantic segmentation (MS-Unet): First, the ostia locations are identified by precomputing the mask of the aorta. Second, next locations are identified by clustering the intersections of the U-Net output with a sphere of fixed diameter adjusted to the receptive field of the Unet model. This is done for a given current location inside the coronary and this process is executed recursively on next locations until the current location is marked as an

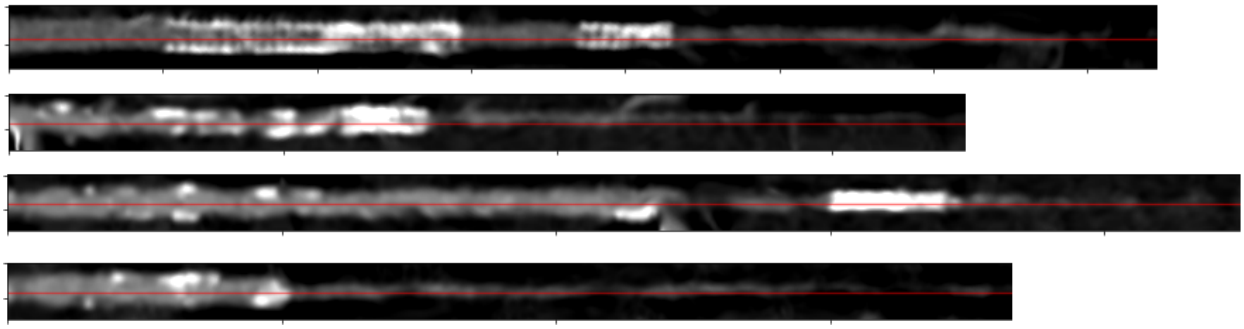

Fig. 4. A sample of extracted centerlines, rough coordinates are used to compute orthogonal frames to inspect the coronary visualized with multi-planar reconstructions at a sub-voxel resolution of $(0.25 \times 0.25 \times 0.25)mm^3$ [13]

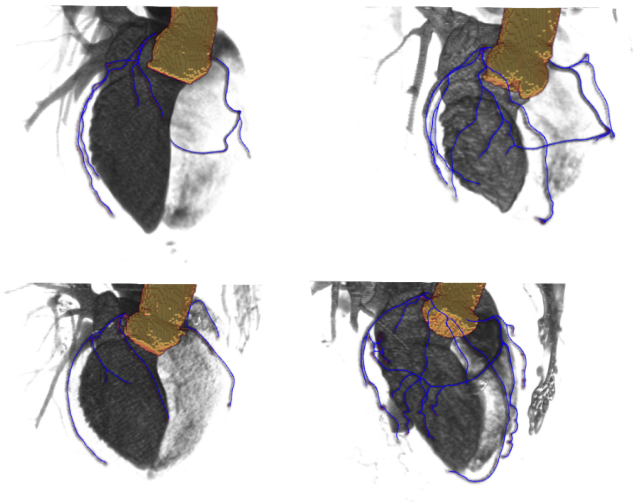

Fig. 5. Recursive tracking output. Blue: coronary centerline extracted. Yellow: Aorta mask.

extremity. The receptive field of the U-Net is large enough to bridge over stenosis. The recursive inference procedure outputs a set of locations, with associated segmentation and extremities. The union of all local segmentation is used to find the minimum cost path from the extremities to the corresponding ostium. All positive voxels of the segmentation output constitutes the nodes and the average U-Net output value as the weight of the edge between 2 voxels (see Fig. 5).

3.2.1. Evaluation

Our dataset employs 225 examinations: 100 for training 55 for validation, and 70 for the test. The test set was chosen by focusing on the clinical use of coronary tracking; most CCTA examinations have severe calcifications and present artifacts or stents, 40 patients presents a > 400 coronary artrey calcium (CAC) score wich is associated with high cardiovascular risk and stenosis among these 12 have stents. The proposed tracking method is evaluated on the test (fig. 3)(tab. 1) against a state-of-the-art deep-learning approach [11]. Predicted centerlines are evaluated with a standard evaluation method [18]. Total overlap (OV), overlap until first error (OF), and overlap of the extracted centerline with the clinically relevant part of the vessel (radius ≥ 0.75 mm, OT) are computed using true positive (TP), false positive (FP) and false-negative (FN) detections. An TP point lies within the radius of the closest manually annotated point. An FP point does not lie within the radius of any manually annotated point. An FN point is a manually annotated centerline point with no corresponding automatically extracted point. The average inside accuracy metric (AI) measures the average distance between the manually annotated and extracted centerline for automatically extracted points.

4. CONCLUSION AND DISCUSSION

This work proposes an improved morphological skeletonization algorithm and a resource-efficient scheme for back-propagation functions involving skeletonization. Our formulation results in a connected skeleton enabling its use in deep-learning semantic segmentation algorithms. The resource efficient scheme is based on the derivative restricted to the morphological skeleton. Moreover, this approximation opens up new possibilities to exploit even better skeletonization algorithms that could improve the quality of the results. The proposed method rivals the deep-learning state-of-the-art method for coronary tracking and shows promising results on clinically relevant CCTA examinations; our test dataset has complete coronary annotations with more than 600 annotated centerlines and comprises mostly examinations with severe calcifications and stents (fig. 4). While this method has been implemented for a fixed voxel resolution of 0.4 *mm*, an improvement would be necessary to achieve sub-voxel resolution. Although prior use of a U-Net [7] our work proposes a taylored and effective implementation of a deep learning vessel centerline semantic sementation method using the centerline alone as supervision.

5. REFERENCES

[1] Jonathon Leipsic, Suhny Abbara, Stephan Achenbach, Ricardo Cury, James P. Earls, GB John Mancini, Koen Nieman, Gianluca Pontone, and Gilbert L. Raff, "SCCT guidelines for the interpretation and reporting of coronary CT angiography: A report of the Society of Cardiovascular Computed Tomography Guidelines Committee," *Journal of Cardiovascular Computed Tomography*, vol. 8, no. 5, pp. 342–358, Sept. 2014.

[2] Karl Krissian, Hrvoje Bogunovic, Hrvoje Bogunovic, Jose Maria Pozo, Maria Cruz Villa-Uriol, and Alejandro Frangi, "Minimally Interactive Knowledge-based Coronary Tracking in CTA using a Minimal Cost Path," *The MIDAS Journal*, July 2008.

[3] Ro Frangi, W.J. Niessen, Koen Vincken, and Max Viergever, "Multiscale vessel enhancement filtering," *Med. Image Comput. Comput. Assist. Interv.*, vol. 1496, 02 2000.

[4] Odyssee Merveille, Hugues Talbot, Laurent Najman, and Nicolas Passat, "Curvilinear Structure Analysis by Ranking the Orientation Responses of Path Operators," *IEEE Transactions on Pattern Analysis and Machine Intelligence*, vol. 40, no. 2, pp. 304–317, Feb. 2018.

[5] Odyssee Merveille, Benoit Naegel, Hugues Talbot, and Nicolas Passat, "n D Variational Restoration of Curvilinear Structures With Prior-Based Directional Regularization," *IEEE Transactions on Image Processing*, vol. 28, no. 8, pp. 3848–3859, Aug. 2019.

[6] Amos Sironi, Engin Turetken, Vincent Lepetit, and Pascal Fua, "Multiscale Centerline Detection," *IEEE Transactions on Pattern Analysis and Machine Intelligence*, vol. 38, no. 7, pp. 1327–1341, July 2016.

[7] Alexandru Dorobanțiu, Valentin Ogrean, and Remus Brad, "Coronary Centerline Extraction from CCTA Using 3D-UNet," *Future Internet*, vol. 13, no. 4, pp. 101, Apr. 2021.

[8] Ruochen Gao, Zhihui Hou, Jun Li, Hu Han, Bin Lu, and S. Kevin Zhou, "Joint Coronary Centerline Extraction And Lumen Segmentation From Ccta Using Cntracker And Vascular Graph Convolutional Network," in *2021 IEEE 18th International Symposium on Biomedical Imaging (ISBI)*, Nice, France, Apr. 2021, pp. 1897–1901, IEEE.

[9] Byunghwan Jeon, "Deep Recursive Bayesian Tracking for Fully Automatic Centerline Extraction of Coronary Arteries in CT Images," *Sensors*, vol. 21, no. 18, pp. 6087, Sept. 2021.

[10] Geert Litjens, Francesco Ciompi, Jelmer M. Wolterink, Bob D. de Vos, Tim Leiner, Jonas Teuwen, and Ivana Išgum, "State-of-the-Art Deep Learning in Cardiovascular Image Analysis," *JACC: Cardiovascular Imaging*, vol. 12, no. 8, pp. 1549–1565, Aug. 2019.

[11] Jelmer M. Wolterink, Robbert W. van Hamersvelt, Max A. Viergever, Tim Leiner, and Ivana Išgum, "Coronary artery centerline extraction in cardiac CT angiography using a CNN-based orientation classifier," *Medical Image Analysis*, vol. 51, pp. 46–60, Jan. 2019.

[12] Suprosanna Shit, Johannes C. Paetzold, Anjany Sekuboyina, Ivan Ezhov, Alexander Unger, Andrey Zhylka, Josien P. W. Pluim, Ulrich Bauer, and Bjoern H. Menze, "clDice - a Novel Topology-Preserving Loss Function for Tubular Structure Segmentation," in *2021 IEEE/CVF Conference on Computer Vision and Pattern Recognition (CVPR)*, Nashville, TN, USA, June 2021, pp. 16555–16564, IEEE.

[13] Armin Kanitsar, Dominik Fleischmann, and Rainer Wegenkittl, "Diagnostic Relevant Visualization of Vascular Structures," in *Scientific Visualization: The Visual Extraction of Knowledge from Data*, Georges-Pierre Bonneau, Thomas Ertl, and Gregory M. Nielson, Eds., pp. 207–228. Springer-Verlag, Berlin/Heidelberg, 2006.

[14] Imen Melki, Cyril Cardon, Nicolas Gogin, Hugues Talbot, and Laurent Najman, "Learning-based automatic detection of severe coronary stenoses in CT angiographies," San Diego, California, USA, Mar. 2014, p. 903536.

[15] Laurent Najman and Hugues Talbot, Eds., *Mathematical Morphology: From Theory to Applications*, John Wiley & Sons, Inc., Hoboken, NJ, USA, Feb. 2013.

[16] H. Blum, "A transformation for extracting new descriptors of shape," in *Models for Perception of Speech and Visual Form*, W. Wathen-Dunn, Ed. MIT Press, Cambridge, MA, 1967.

[17] Herbert Edelsbrunner and J. Harer, *Computational topology: an introduction*, American Mathematical Society, Providence, R.I, 2010, OCLC: ocn427757156.

[18] Michiel Schaap, Coert T. Metz, Theo van Walsum, Alina G. van der Giessen, Annick C. Weustink, Nico R. Mollet, Christian Bauer, Hrvoje Bogunović, Carlos Castro, and Xiang Deng, "Standardized evaluation methodology and reference database for evaluating coronary artery centerline extraction algorithms," *Medical Image Analysis*, vol. 13, no. 5, pp. 701–714, Oct. 2009.